IJIE

UTHM Penerbit
Universiti Tun Hussein Onn Malaysia

INTERNATIONAL JOURNAL OF INTEGRATED ENGINEERING
ISSN: 2229-838X e-ISSN: 2600-7916

Vol. 18 No. 3 (2026) 243-256
https://publisher.uthm.edu.my/ojs/index.php/ijie

The Correlation Between Electrical Resistivity Tomography and Borehole Data at a Coastal Semi-Developed Area

Z. M. Nizam[1]*, H. Obiya[1], A. T. S. Azhar[2,5], Z. M. N. Hidayat[3], M. Aziman[2], J. Amir[2], I. M. Fakhrurrazi[4]

[1] *Faculty of Science and Engineering, Saga University, Honjo 1, 840-8502, Saga, JAPAN*
[2] *Faculty of Civil Engineering and Built Environment, Universiti Tun Hussein Onn Malaysia, 86400 Parit Raja, Johor, MALAYSIA*
[3] *Southern Stars Solutions Pte. Ltd., Taman Pura Kencana, 83300 Sri Gading, Johor, MALAYSIA*
[4] *Faculty of Civil Engineering Technology, Universiti Malaysia Pahang Al-Sultan Abdullah, Paya Besar, MALAYSIA*
[5] *Geo-Structure Rehabilitation Centre, Universiti Tun Hussein Onn Malaysia, 86400 Parit Raja, Johor, MALAYSIA*

*Corresponding Author: zmnizam@cc.saga-u.ac.jp
DOI: https://doi.org/10.30880/ijie.2026.18.03.016

Article Info

Received: 21 August 2025
Accepted: 14 April 2026
Available online: 30 April 2026

Keywords

Electrical resistivity tomography, standard penetration test, borehole, subsurface characterization, coastal geophysics

Abstract

This study explores the correlation between Electrical Resistivity Tomography (ERT) and borehole (borelog) data to characterize subsurface properties at a coastal semi-developed area in Melaka, Malaysia. The objective is to assess how resistivity values correspond to soil or rock information obtained from boreholes, with a focus on geological features, material types, and groundwater levels. A strong linear correlation (R^2 = 0.93) was established between resistivity values and SPT N-values, especially where ERT lines were closely aligned with borehole locations. The research evaluates the reliability and applicability of ERT as a non-destructive method, comparing it to traditional point-based techniques like the Standard Penetration Test (SPT). By integrating continuous ERT profiles with borehole data, the study addresses trade-offs in resolution and accuracy between these methods. Results show a strong correlation between resistivity and SPT N-values, particularly in areas where ERT lines were closely aligned with boreholes. The findings highlight the applicability of ERT as a complementary tool for preliminary geotechnical investigation and slope or coastal site assessment in urban and geologically complex environments.

1. Introduction

Subsurface investigation is a critical component of construction and civil engineering projects, as soil and rock conditions can vary significantly over short distances and time [1]. The Standard Penetration Test (SPT) is widely used for determining soil strength and classification, yet it provides data only at discrete points, making it laborintensive, time-consuming, and sometimes insufficient for complex geological settings [2], [3]. Electrical Resistivity Tomography (ERT) offers a non-invasive alternative capable of mapping subsurface structures over a continuous profile [4] – [8]. It is particularly effective in identifying geological features, groundwater levels, and soil variations due to its sensitivity to differences in electrical resistivity, which depends on factors like moisture content, mineral composition, and soil texture [2], [9] – [11].

While SPT provides direct measurements of soil resistance to penetration (N-values), it is subject to variability from human error and equipment inconsistencies [12]. Conversely, ERT measures electrical conductivity indirectly through electrode arrays, offering broad spatial coverage [14]. In coastal regions, the salinity and moisture content in soils can significantly influence the correlation between SPT N-values and resistivity measurements [2], [13], [15], [16]. In previous study, Sudha *et al.* [17] emphasized that the relationship between ERT and SPT is highly site-specific. However, despite increasing applications of ERT in Malaysia, limited studies have quantitatively established resistivity–SPT correlations in coastal or semi-developed zones, particularly in Melaka, where saline influence and heterogeneous subsurface conditions may alter geophysical responses; most existing research focuses on inland residual soils or generalized empirical relationships without detailed site-specific validation. Therefore, a clear research gap exists in evaluating the reliability of ERT for preliminary geotechnical investigation in Malaysian coastal environments. This research aims to establish such a correlation for the Terendak area in Malacca by analyzing data from ERT profiles and two boreholes using regression analysis, contributing a quantitative assessment of the resistivity–SPT relationship, establishing a site-specific regression model to evaluate correlation strength, and demonstrating the applicability of ERT as a complementary tool for preliminary geotechnical and coastal site investigation [18], [19].

2. Study Area

Environmental factors were considered during the meticulous planning phase, including the possibility of the presence of geological faults and the complex lithological formations that can affect resistivity readings due to variations in subsurface properties. The study area is located in Terendak, Malacca state of Malaysia and is characterized by regional geology dominated primarily by coarse-grained biotite granite, consisting mainly of quartz, feldspar, and mica minerals, as shown in Fig. 1 [20]. Geomorphologically, the area lies near coastal landforms (Fig. 2) and is interspersed with man-made structures, reflecting significant urban development. It features a mix of developed zones and natural or landscaped green spaces (Fig. 3). The study site includes a steep coastal slope where slope failure occurred between 82.5 and 100 m along the survey line (Fig. 4). The slope measures approximately 6 m in height, 15 m in width, and has an angle of 25 degrees.

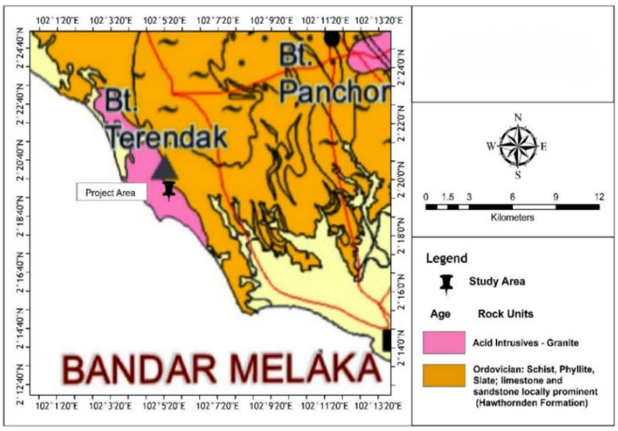

Fig. 1 *Location of the geological study area in Malacca*

Fig. 2 *Coastal landform*

Fig. 3 *Vegetations at the P.O. I*

Fig. 4 *Slope failure along the survey line*

This study utilized the ABEM Terrameter LS2, an advanced instrument designed for measuring subsurface electrical resistivity. The equipment integrates seamlessly with ERT to accurately detect variations in subsurface electrical properties, aiding in the identification of rock types, soil composition, and groundwater presence. The multi-electrode system enabled efficient data collection across the site locations, thereby enhancing the spatial coverage of the survey. The layout of each survey line was carefully planned, taking into account geological composition, topographic elevation, site accessibility, guidance from reference materials.

Here, two 200 m long survey lines were deployed using the Gradient XL protocol to investigate subsurface conditions up to a depth of 40 m. The locations of two SPT boreholes and two ERT lines are shown in the diagram, with each ERT line positioned strategically near its corresponding SPT borehole to facilitate data comparison. This layout, often adopted in major geotechnical and geophysical investigations, enhances the correlation between methods [21], [22]. The collected data were then processed into pseudo cross-sections to visualize the subsurface conditions at each proposed site.

3. Methodology

This study employed two complementary methods to investigate subsurface conditions: the SPT and ERT. The SPT was used to obtain in-situ measurements of soil strength and collect soil samples, providing critical information on geotechnical properties such as relative density, consistency, and bearing capacity. In parallel, the ERT method was applied to measure variations in electrical resistivity within the subsurface, offering insights into soil composition, moisture content, and the presence of groundwater. Following data acquisition, the results from both methods were analyzed collectively. The electrical resistivity profiles generated by the ERT survey were correlated with the geotechnical data obtained from the SPT, particularly focusing on the relationship between resistivity values and soil strength parameters such as N-values.

The apparent resistivity data were processed using inversion software to generate two-dimensional resistivity models, with final root mean square (RMS) errors ranging between 12% and 14.6%. These RMS values are considered acceptable for coastal terrains, where heterogeneous sediments, saline groundwater intrusion, and near-surface moisture variations commonly increase inversion uncertainty, and are within the generally acceptable range for near-surface geophysical investigations. Following inversion, resistivity values were extracted at depths corresponding to SPT test intervals to ensure consistent depth matching. A total of regression data points was obtained by pairing averaged resistivity values from the inverted ERT sections with corresponding SPT N-values at matching depth ranges, with depth correlation based on the closest vertical alignment between borehole positions and ERT profiles.

By comparing these datasets, the study aimed to establish a meaningful correlation between electrical resistivity and geotechnical strength characteristics. Identifying such a correlation is essential to the primary objective of this research, which is to enhance the interpretation of resistivity data by integrating it with conventional geotechnical testing. This integrated approach can improve the accuracy and reliability of subsurface investigations, ultimately supporting better-informed decisions in site characterization, construction planning, and groundwater resource assessment.

3.1 Standard Penetration Test (SPT)

The SPT is one of the most widely used in-situ testing methods in geotechnical engineering, providing critical information about subsurface conditions. This test plays a fundamental role in site investigation by offering valuable data on soil stratigraphy, soil classification, and the depth and position of the groundwater table. Its simplicity, cost-effectiveness, and reliability have made it a cornerstone technique in preliminary site assessment for construction, foundation design, and geotechnical research. The SPT process involves a systematic three-stage procedure:

1. **Drilling**: A borehole is drilled into the ground using a rotary or percussion rig to reach the desired testing depth. Casing is often used to prevent borehole collapse and groundwater intrusion.
2. **Penetration Testing**: A standard split-barrel sampler (also known as a split-spoon sampler) is driven into the soil at the bottom of the borehole using a 63.5 kg hammer dropped from a height of 760 mm. The sampler is driven in three successive 150 mm increments, totaling 450 mm. The first 150 mm is considered a seating drive, and the number of blows required to drive the sampler through the next 300 mm is recorded as the SPT N-value or blow count.
3. **Sampling**: After the penetration is complete, the sampler is retrieved, and the soil contained within is extracted for visual classification and, if necessary, laboratory testing.

The resulting SPT N-value represents the resistance index to dynamic penetration, reflecting the relative density or consistency of the soil. Higher N-values typically indicate denser sands or stiffer clays, while lower values suggest loose or soft soil conditions. This resistance index is a fundamental parameter in geotechnical engineering, used for estimating bearing capacity, settlement potential, and liquefaction susceptibility. In this study, the SPT procedure was conducted in accordance with the British Standard BS 1377:1990 — Methods of Test for Soils for Civil Engineering Purposes. This standard ensures the consistency, accuracy, and comparability of results, particularly in deep lithological investigations. Data derived from the SPT were instrumental in profiling the subsurface lithology and validating results obtained through geophysical methods such as ERT. In addition, SPT also allows for the estimation of groundwater level, as water ingress into the borehole can be monitored during drilling. The detection of the water table is crucial for evaluating foundation safety, particularly in coastal or flood-prone regions, where soil strength and water saturation are strongly correlated.

3.2 Electrical Resistivity Tomography (ERT)

ERT is a non-invasive geophysical imaging technique that provides high-resolution, two-dimensional (2D) representations of subsurface resistivity variations. As shown in Fig. 5, this method operates by injecting electrical current into the ground and measuring the resulting potential differences at the surface. Through measurements taken at various electrode positions and depths, the ERT method constructs discrete data points that, when interpolated using inversion algorithms, generate continuous 2D tomographic images (Fig. 6). These images display the lateral and vertical distribution of subsurface resistivity, thereby enabling the identification of variations in lithology, water content, porosity, and saturation zones.

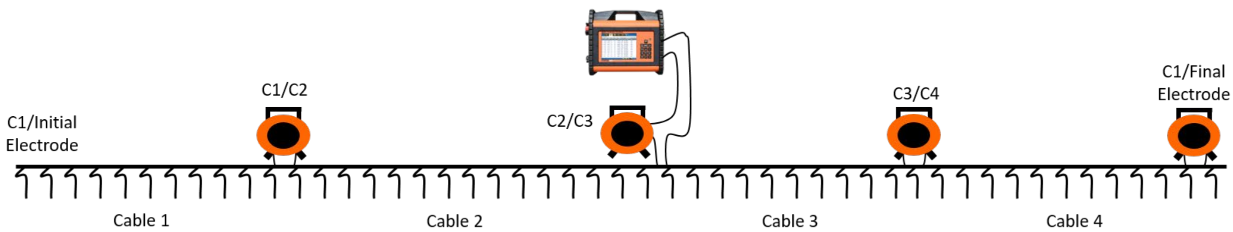

Fig. 5 *Schematic of ERT electrode configuration*

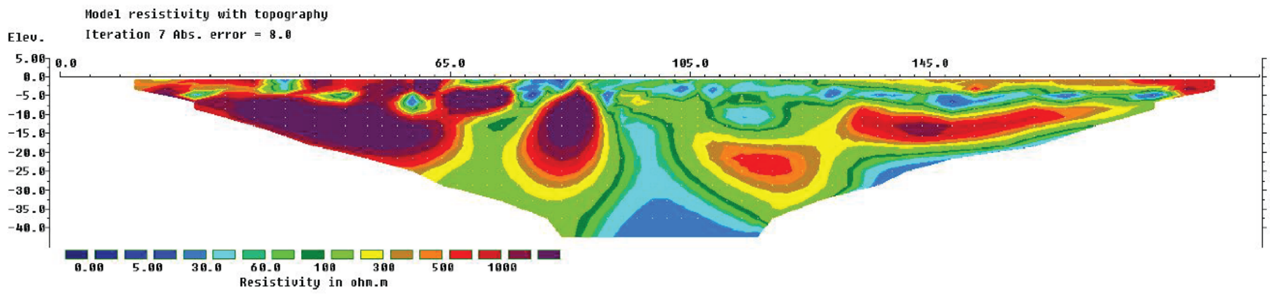

Fig. 6 *Example of 2D ERT pseudo-section and inverted resistivity model*

The ERT system utilizes two current electrodes (C1 and C2) to introduce a continuous electrical current into the subsurface (Fig. 7). Simultaneously, two potential electrodes (P1 and P2) measure the resulting voltage difference at the ground surface [23]. This voltage response is influenced by the electrical resistivity of the materials through which the current flows. According to Ohm's Law and the principles of potential field theory, the resistivity (ρ) can be calculated based on the injected current, measured voltage, and geometric factors related to electrode spacing [24]. The acquired point measurements are processed using inversion software to produce pseudo-sections, which are further refined into true resistivity models. As shown in Fig. 8, these models are capable of delineating features such as aquifers, bedrock interfaces, and contaminant plumes with greater clarity than traditional 1D methods.

In this study, two ERT lines (designated RL01 and RL02) were deployed in close proximity to previously drilled boreholes. This spatial alignment was intentional, allowing for direct correlation between geophysical (ERT) and geotechnical (borehole) data, enhancing the accuracy of subsurface interpretation. The maximum electrode spacing for both lines was 1.62 m, while the minimum was 1.37 m, carefully selected to balance resolution and depth of investigation. The survey lines were oriented according to site-specific parameters, including topography, access routes, and known geological features.

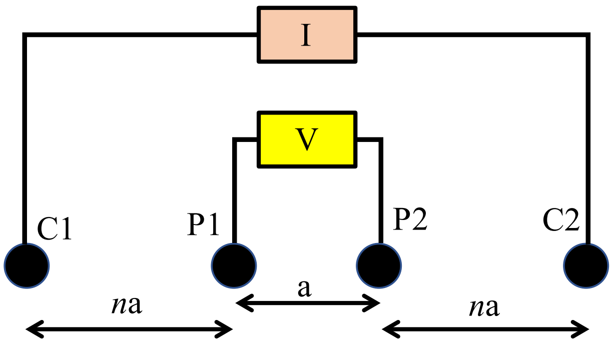

Fig. 7 *Gradient-XL array diagram*

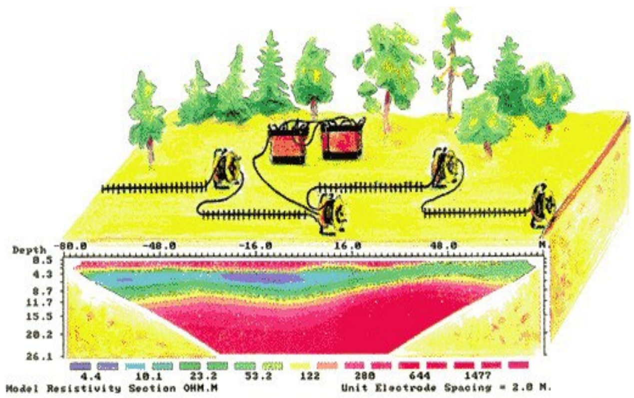

Fig. 8 *Field setup with ABEM Terrameter LS 2*

The Gradient XL array protocol was utilized, which operates similarly to the traditional Schlumberger array. This configuration records voltage measurements across multiple adjacent dipole pairs between two transmitting electrodes, significantly increasing the density and depth of data acquisition. The Gradient XL protocol is particularly effective in detecting horizontal layering and vertical structures, making it suitable for environments with complex stratigraphy or variable resistivity zones. The choice of this array configuration was influenced by the expected geological setting and the resolution required to delineate specific features. As emphasised by Sufiyanussuari *et al.* [25], array selection must align with both the anticipated resistivity contrasts and the spatial geometry of the target subsurface structures.

All resistivity measurements were conducted using the ABEM Terrameter LS 2, a state-of-the-art resistivity imaging system known for its versatility and field robustness. The device features 12 measurement channels and a built-in electrode selector, enabling automatic switching among up to 81 electrodes. This configuration enhances field productivity and data quality by minimizing downtime between measurements and allowing deeper investigations with high lateral resolution (Fig. 8). The placement of electrode cables was determined by precise measurements from the first electrode to the central LS unit and subsequently to the last electrode, taking into account the total profile length as specified in Table 1. These measurements ensured proper electrode positioning, accurate data collection, and full coverage of the target area.

Table 1 *Distance of electrode cable according to profile lines length*

Profile Length(m)	C1/ Initial electrode - C1/C2(sharing)	C1/C2 (sharing) – C2/C3 (Center)	C2/C3 (Center) - C3/C4(sharing)	C3/C4 (sharing) – C4/ Last electrode
200	50m	100m	150m	200m

3.3 Data Processing

To process and interpret the electrical resistivity data collected during the field survey, RES2DINV and ZondRes2D software were utilized. These programs perform two-dimensional (2D) inversion of apparent resistivity measurements, transforming raw field data into meaningful subsurface resistivity models. The inversion process plays a critical role in interpreting geophysical surveys by estimating the true resistivity distribution from the apparent resistivity values recorded during the ERT survey. The inversion software generates a 2D subsurface model, composed of a mesh of rectangular elements (blocks). Each block represents a discrete unit of subsurface material with an assigned resistivity value. These values are calculated using the least-squares inversion method, an iterative numerical approach that minimizes the difference between the measured apparent resistivity and the calculated resistivity from the model [17]. The objective function in this optimization balances data misfit with model smoothness, ensuring geologically plausible outcomes. The output from this inversion process typically includes three distinct resistivity sections:

1. Measured apparent resistivity pseudo-section: Represents raw field data plotted against electrode positions and depth levels.
2. Calculated apparent resistivity section: Illustrates the forward model prediction of resistivity, based on the initial inversion output.
3. Inverted resistivity model (True Resistivity Section): Depicts the final resistivity distribution obtained after multiple iterations, interpreted as the best approximation of the true subsurface structure.

Table 2 *Color-coded resistivity scale*

Resistivity value (Ωm)	*Legend*	Interpretation
1 to 100	0.00 5.00 30.0 60.0 100	Zone of soil / rock saturated with water
>100	300 500 1000 4000	Zone of rock / soil of less saturated with water

Table 3 *Resistance of soil or rock types in the study area [28]*

Soil/ Rock Type	Resistivity value (Ω m)
Alluvium	10 to 800
Sand	60 to 1,000
Clay	1 to 100
Groundwater (fresh)	10 to 100
Sandstone	8 to 4,000
Shawl	20 to 2,000
Slate/ quartz mica schist	500 to 50,000
Graphite schist	10 to 500
Limestone	50 to 4,000
Granite	50 to 10,000

To quantify the accuracy of the inversion, Root Mean Square (RMS) error values are computed. The RMS error expresses the average discrepancy between the measured and calculated apparent resistivity values. A low RMS value (typically below 5%) indicates a good fit between the model and observed data. However, extremely low RMS values might reflect overfitting and should be interpreted alongside geological plausibility. The final inverted resistivity model is interpreted by integrating it with ground truth geological data obtained from boreholes and Standard Penetration Test (SPT) results. As shown in Table 2, the resistivity values are color-coded using a continuous scale, where each color band corresponds to a specific resistivity range. These ranges are typically classified based on standard reference values for common subsurface materials [25], as shown in Table 3.

These classifications help in delineating lithological boundaries, identifying aquifer zones, and assessing subsurface anomalies, such as voids or contamination plumes. The resistivity contour maps generated through inversion are then refined using geological input to improve interpretive accuracy. Reference values for typical resistivity ranges are derived from established geophysical literature and field calibration [25].

3.4 Correlating Both SPT-N and ERT

To evaluate the relationship between geotechnical properties and geophysical responses, a least squares regression approach was employed. This statistical method is commonly used in geophysical studies to identify and quantify correlations between parameters such as electrical resistivity and soil strength Melvern *et al.* [27]. The aim was to establish empirical relationships that allow for indirect estimation of geotechnical parameters, specifically, the SPT-N values, based on resistivity data derived from ERT surveys. A qualitative and quantitative comparative analysis was conducted to assess the alignment between ERT-derived resistivity measurements and lithological classifications obtained from SPT borehole data. For this purpose, ERT resistivity values at depths corresponding to SPT N-value measurements were extracted at each borehole location. These paired datasets were subjected to linear regression analysis, allowing for the development of correlation equations for each individual borehole.

Moreover, to improve the reliability and site-specific relevance of these correlations, additional resistivity and SPT data were collected from adjacent boreholes exhibiting similar lithological composition and positioned at comparable depths relative to the groundwater table. This stratified approach ensured that the correlation models reflected consistent geological and hydrogeological conditions across the study area. The correlation between electrical resistivity and geotechnical strength is highly site-dependent Sudha *et al.* [17], largely influenced by local soil type, moisture content, clay fraction, and degree of weathering. Once a reliable relationship is established for a specific region, ERT-derived resistivity profiles can serve as proxies for estimating soil strength, particularly in areas where direct sampling is limited or inaccessible.

Further analysis was conducted to observe the behavior of regression fitting coefficients, especially in relation to changes in lithological composition and clay content. By analyzing how the slope and intercept of the regression lines varied with respect to these geological parameters, the study evaluated the sensitivity and robustness of the derived models. Finally, the fitting parameters (i.e., slope, intercept, and coefficient of determination R^2) were compared with average resistivity values and mean SPT N-values across the study area to assess the predictive quality and consistency of the regression models.

4. Result and Discussion

The findings of this study are interpreted and discussed in the context of the integrated dataset obtained from both geophysical and geotechnical investigations. Specifically, the analysis focuses on elucidating the relationship between ERT results and SPT data. This comparative approach enables a comprehensive understanding of subsurface conditions by correlating resistivity variations with mechanical soil strength parameters. The outcomes demonstrate the extent to which geophysical measurements i.e., particularly resistivity values, can be used as proxies for geotechnical indicators, such as the SPT N-value. This correlation provides valuable insights into subsurface stratigraphy, soil behavior, and material properties without the need for extensive intrusive sampling. As such, the study underscores the effectiveness of combining geophysical and geotechnical methods to enhance the reliability and resolution of subsurface investigations.

Furthermore, the interpretation of results contributes to the broader objective of developing site-specific empirical models, which can facilitate non-invasive soil characterization in future studies or engineering applications. The discussion also addresses the consistency of these findings with previous literature and highlights any site-specific anomalies, limitations, or recommendations for further research.

In coastal environments such as the Terendak area, groundwater salinity plays a significant role in influencing resistivity measurements, as saline pore water reduces bulk resistivity and may amplify contrasts between saturated and unsaturated layers. This effect explains the pronounced low-resistivity zones observed near shallow groundwater levels and highlights the importance of calibrating ERT data with borehole information to avoid misinterpretation. Compared with previous studies conducted in tropical regions such as Brazil and Sumatra, where moderate to strong correlations between resistivity and SPT values were reported in residual and alluvial soils, the correlation obtained in this study falls within the upper range of reported values, likely due to the close spatial alignment between ERT lines and boreholes and careful depth matching procedures. However, the regression model developed here remains site-specific, as resistivity–SPT relationships are influenced by local lithology, moisture conditions, and salinity; therefore, while the model provides a reliable reference for similar coastal terrains, its direct transferability to inland or non-saline environments may require recalibration.

4.1 Geotechnical Investigation (Bore log SPT-N)

The results from two boreholes, referred to as Borehole 1 and Borehole 2, are presented in Fig. 9(a) and (b), which illustrates their respective lithological profiles and associated geotechnical properties. The subsurface profile of Borehole 1 consists primarily of stiff to medium-stiff silty sand with moderate to high plasticity, encountered from depths of approximately 1.50 m to 9.45 m. This soil type, comprising clayey silt and fine sand, is generally suitable for light infrastructure applications, such as road base construction or shallow foundation systems, due to its intermediate load-bearing capacity and relatively stable moisture retention characteristics.

At greater depths, from 10.50 to 15.00 m, high-quality granite bedrock was encountered. The granite was retrieved through core sampling and displayed excellent integrity, making it a potential candidate for anchoring deep foundations or for quarrying purposes. The transition from unconsolidated sediments to bedrock is significant for geotechnical design, particularly in assessing load-bearing strata and excavation feasibility. The Standard Penetration Test (SPT) N-values for Borehole 1 demonstrated a general increase with depth, which is consistent with the natural geostatic stress increase and progressive soil compaction. The maximum N-value recorded was 196 blows, which is indicative of very dense material, typically characteristic of weathered or unweathered rock or compacted gravelly sand.

Importantly, the proximity of Borehole 1 to the ERT survey line allowed for more accurate correlation between resistivity data and borehole lithology. The close spatial alignment enhanced the reliability of the geophysical-geotechnical integration and contributed to the robustness of the correlation models developed in this study. The final groundwater level was measured at 6.11 m below ground surface (BGS), indicating a moderately deep phreatic surface which may influence both resistivity values and soil strength behavior.

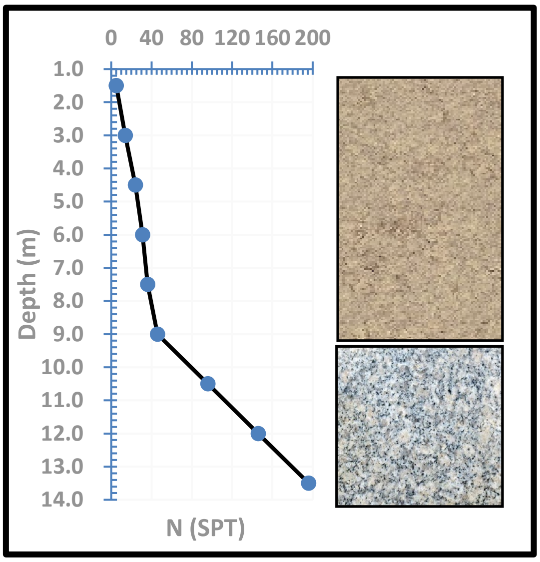

(a) Borehole 1

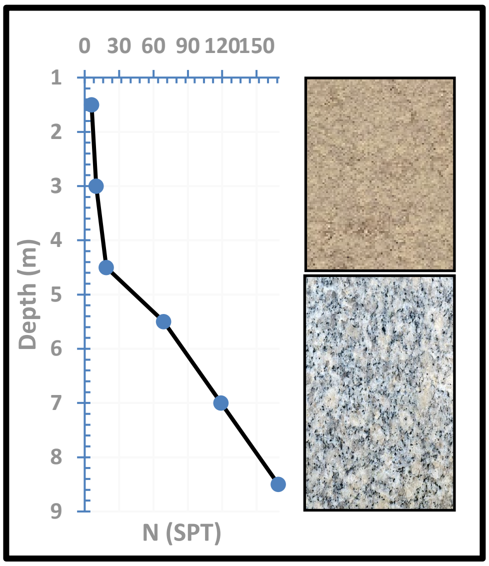

(b) Borehole 2

Fig. 9 *SPT-N results for Borehole 1 and Borehole 2*

Borehole 2 revealed a lithological profile similar to Borehole 1 in its upper layers. From 1.50 to 4.95 m, the subsurface is composed of silty sand, again suitable for light civil engineering applications such as pavement subgrade or shallow footing support. The SPT N-values recorded in this layer reached up to 169 blows, reflecting very dense, competent soil conditions, comparable to those found in Borehole 1. Beneath this layer, at a depth of 5.50 m, granite bedrock was encountered and continued down to 10.00 m. The presence of granite in both boreholes suggests a laterally continuous bedrock formation, which provides critical information for structural foundation planning and slope stability assessments.

In contrast to Borehole 1, the groundwater level in Borehole 2 was recorded at a shallow depth of 0.29 m, implying a higher water table in this area. This variation in hydrogeological condition is likely to affect both the resistivity readings and mechanical behavior of the overlying soils, particularly in finer-grained materials that are sensitive to saturation.

4.2 ERT Results

The classification of subsurface materials in this study is largely informed by their electrical resistivity values, which serve as an indirect indicator of moisture content and material composition. In geophysical investigations, resistivity values below 100 Ωm typically denote saturated conditions, often indicating the presence of water-bearing soils or porous, water-filled rock formations. In contrast, resistivity values exceeding 100 Ωm are generally indicative of unsaturated or drier materials, with lower moisture content and higher grain-to-grain contact resistance. This classification scheme, which is grounded in the empirical work Netto *et al.* [29], is summarised in Fig. 10, and has been applied consistently throughout this study to interpret the resistivity data obtained from the Electrical Resistivity Tomography (ERT) surveys.

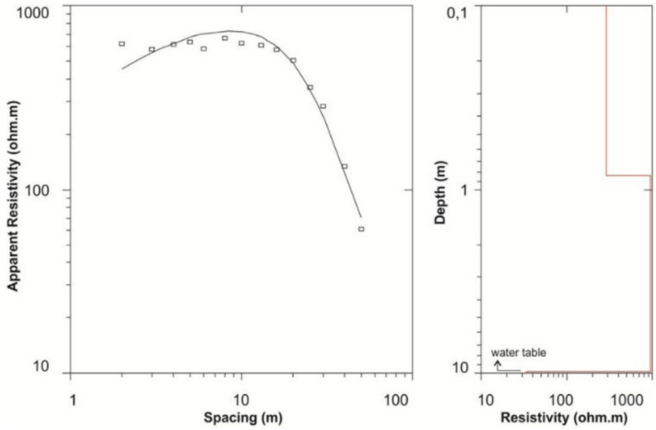

Fig. 10 *Classification of resistivity ranges and corresponding water content* [29]

The resistivity data were carefully processed, with negative values and anomalous outliers removed to ensure data quality and model accuracy. The clean dataset was then subjected to 2D inversion using RES2D and ZondRes2D software, generating inverted resistivity models that allow for detailed visualization of subsurface resistivity variation along two survey lines, RL01 and RL02. Fig. 11 illustrates the inverted resistivity model for survey line RL01. The model reveals that the majority of the subsurface to a depth of 40 m exhibits high resistivity values exceeding 100 Ωm, suggesting relatively dry or unsaturated conditions throughout the upper and lower layers. These resistive zones are typically associated with granite bedrock or coarse-grained soils with low moisture retention, which corresponds well with the lithological descriptions from adjacent borehole data. Notably, a granite formation is inferred at a depth of approximately 15 m, supported by both geophysical resistivity values and borehole core descriptions.

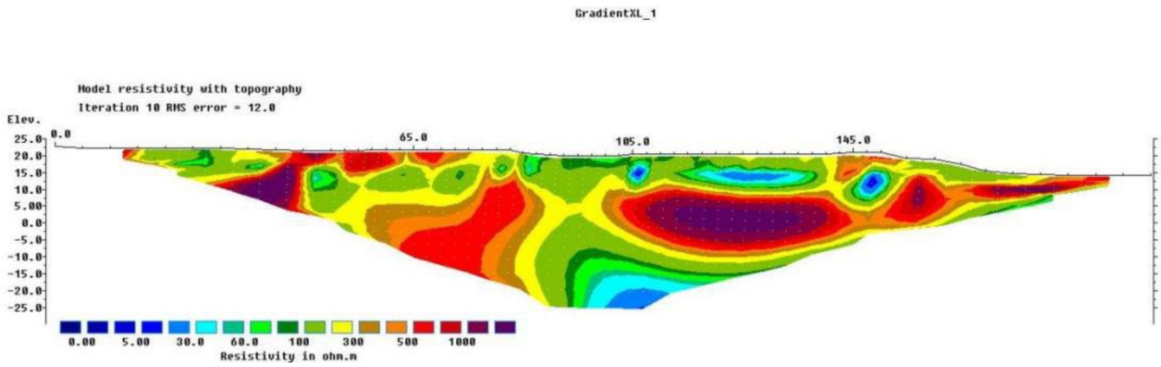

Fig. 11 *Inverted resistivity model for survey line RL01*

The upper 10 m of the profile exhibit more variation in resistivity, likely reflecting heterogeneous surface materials, including sandy silt with clay admixtures. Despite lithological differences, these layers display similar resistivity responses due to comparable moisture content and mineralogical composition. A notable anomaly is observed between the 80–100 m mark along the survey line, where resistivity values drop below 100 Ωm, with localized zones showing values as low as 0–50 Ωm. These low-resistivity zones strongly suggest water saturation and possibly the presence of shallow groundwater accumulation. Importantly, this saturated zone aligns with the observed location of slope failure, which occurred between 82.5 and 100 m, implying a strong correlation between increased pore water pressure and reduced slope stability.

Fig. 12 presents the resistivity model for survey line RL02, where the subsurface resistivity ranges from 0 to 1000 Ωm. The profile is dominated by resistivity values above 100 Ωm, especially in deeper sections, indicating that this area is composed of less saturated soils or weathered bedrock, similar to RL01. The deeper parts of the profile show a progressive increase in resistivity with depth, consistent with compacted or lithified geological units that possess limited water retention capacity. Although some localized low-resistivity zones are present in the shallower regions, these are less pronounced than those in RL01, suggesting that RL02 lies in a relatively drier zone. This supports the site-specific hydrogeological variability indicated by borehole water level data, where RL02 is associated with a higher elevation and deeper water table.

The resistivity dataset underwent rigorous preprocessing to eliminate errors such as negative readings and anomalously high or low values that could distort the inversion results. A summary of the data before and after processing is provided in Table 3, illustrating the significant improvement in data quality following the application of filtering and cleaning protocols. This process enhanced the reliability of the inverted models and ensured the accurate interpretation of subsurface conditions.

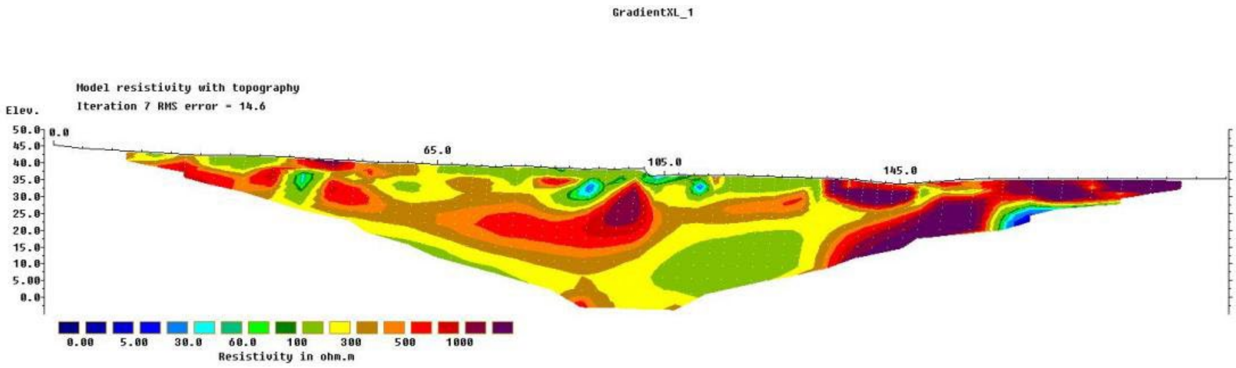

Fig. 12 *Inverted resistivity model for survey line RL02*

Table 3 *Summary of resistivity data points before and after processing*

Profile Line	Number Of Original Data	Negative Data	Excluded Data	Total data post- analysis	RMS Error (%)
RL 1	1030	-1	30	999	12
RL 2	1030	-1	18	1011	14.6

4.3 Correlation of ERT with SPT-N Data

The correlation between the interpreted resistivity values obtained from ERT and the borehole data acquired through SPT investigations is illustrated in Fig. 13. The results demonstrate a strong linear relationship between the electrical resistivity and the SPT N-values within the study area, with the derived regression equation expressed as:

$$y = 0.47x - 63.04 \tag{1}$$

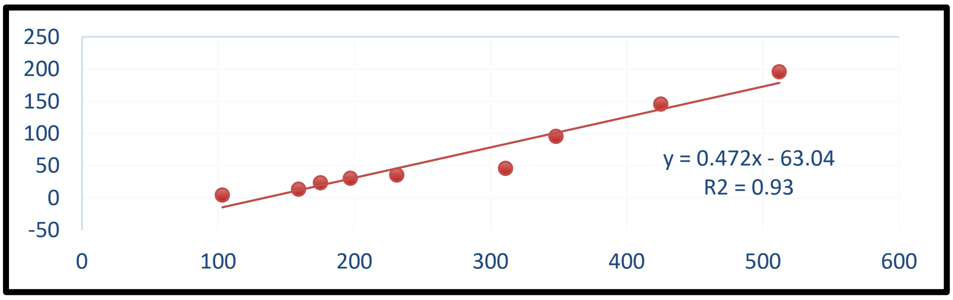

Fig. 13 *Linear relationship between SPT-N vs resistivity (Ωm)*

In this expression, y denotes the SPT N-value, and x represents the resistivity (Ωm). The correlation coefficient (R) for this linear relationship is 0.93, indicating a very high degree of correlation between the two datasets. Such a high correlation value suggests that electrical resistivity is a reliable proxy for estimating subsurface strength parameters, particularly in soils and shallow rock where SPT data are often sparse. The level of correlation can be interpreted as an indicator of consistent lithological conditions across the site [17] and Devi *et al.* [30], where variations in resistivity closely mirror the changes in soil and rock strength.

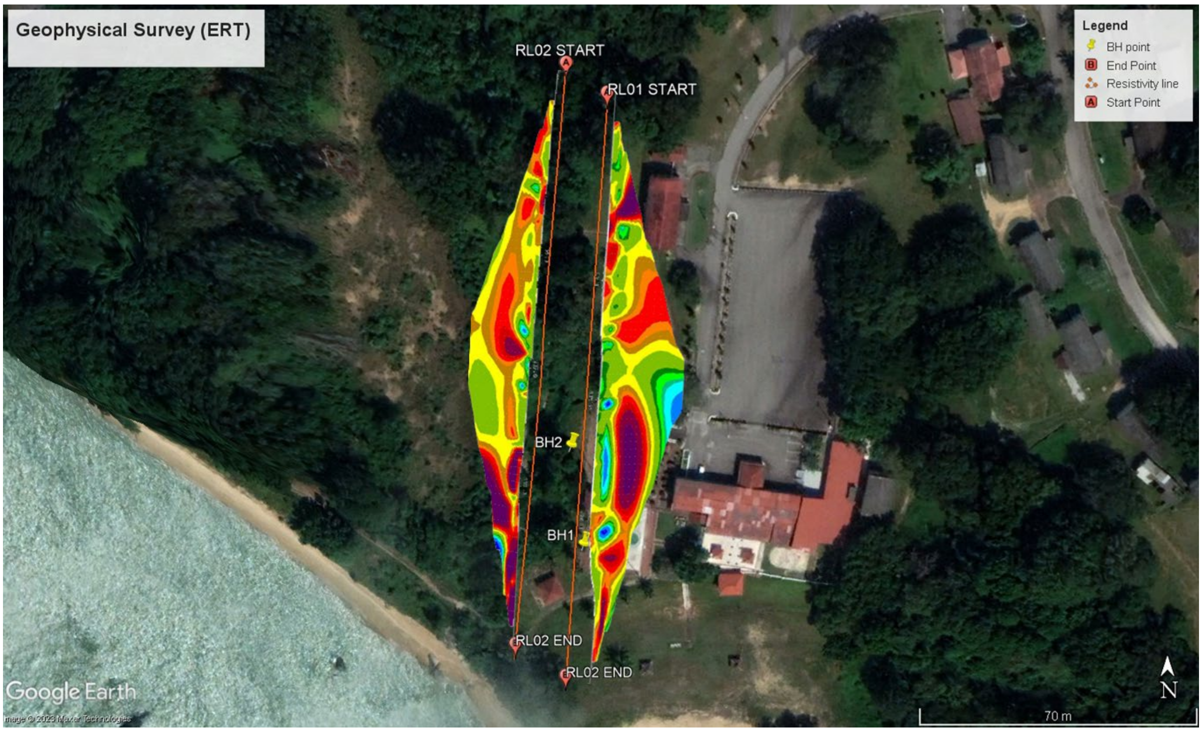

Fig. 14 *ERT overlay on the study area*

The slope of the regression line (0.472) reflects the sensitivity of SPT N-values to changes in resistivity. A higher slope value implies that relatively small variations in resistivity correspond to more significant differences in soil resistance, thus enhancing the diagnostic utility of ERT for geotechnical applications. However, it is important to note that any derived negative resistivity values from the regression model lack physical meaning, as electrical resistivity cannot assume negative quantities in natural materials. Such anomalies are typically attributed to extrapolation errors or data outliers and should be excluded from interpretative conclusions.

The correlation analysis between the resistivity profile RL01 and Borehole 1 further supports these findings. In the upper 10 m of the subsurface, the ERT data reveal low resistivity values (<100 Ωm), corresponding to layers composed primarily of silty sand. This lithology is typically associated with relatively low SPT N-values ranging from 5 to 10, indicating weaker or less compacted soil. Beyond this depth, from approximately 10 m to 25 m, the resistivity values significantly increase, exceeding 100 Ωm. This increase in resistivity aligns well with the borehole data, which confirms the presence of a granite bedrock layer extending to a depth of approximately 15 m. The high resistivity observed in this depth range is characteristic of igneous rock formations, such as granite, which are generally dry, compact, and electrically resistive (Fig. 14). This strong agreement between geophysical and geotechnical data reinforces the applicability of ERT as a non-invasive technique for preliminary subsurface investigations, especially in contexts where borehole drilling is limited due to cost or accessibility constraints.

5. Conclusion

The application of geophysical methods, particularly Electrical Resistivity Tomography (ERT), has proven to be a valuable complement to traditional geotechnical investigations. While geophysical techniques offer an efficient means of acquiring continuous subsurface data across extensive areas, they are indirect in nature and, by themselves, may not provide the detailed resolution necessary for comprehensive geological or geotechnical characterization. Conversely, conventional methods, such as the Standard Penetration Test (SPT), provide highly localized, point-specific data on subsurface stratigraphy and mechanical properties. However, they are constrained by limited spatial coverage and logistical challenges, especially in large or inaccessible terrains.

Geological and geotechnical surveys, when combined with ERT, offer a more holistic understanding of subsurface conditions. While borehole logging and SPT provide precise lithological data at specific depths and locations, ERT facilitates a broader interpretation of the subsurface by measuring variations in electrical resistivity over both lateral and vertical extents. These measurements can indicate the presence of groundwater, changes in lithology, and the depth to bedrock, thereby addressing spatial discontinuities inherent in borehole data. The results from this study demonstrate the synergistic value of integrating SPT with ERT. For instance, SPT data offer quantitative insight into the mechanical strength of soils through the N-value, while ERT models delineate the spatial distribution of subsurface features. By superimposing resistivity data over borehole locations, the study was able to identify zones of correlation between resistivity anomalies and specific soil types, thereby improving interpretive accuracy.

The primary objective of this investigation is to establish a correlation between electrical resistivity and SPT N-values was successfully achieved. The subsurface profile in the study area is generally characterized by high resistivity values exceeding 100 Ωm down to a depth of 40 m, suggesting dry conditions and the possible presence of competent soil or rock layers. In the specific case of survey line RL01 and Borehole 1, lower resistivity values were observed in the upper 10 m, which coincide with silt and fine sand layers identified through borehole sampling. These layers also corresponded to low SPT N-values ranging from 5 to 10, indicative of loose to medium-dense soils. Below this zone, resistivity values increased substantially, reaching levels consistent with granite bedrock identified in borehole cores at depths of 10 to 25 m. These layers also displayed significantly higher N-values, confirming higher material strength and reduced moisture content.

This correlation underscores the effectiveness of ERT in augmenting borehole data, offering spatial continuity where traditional borehole sampling may be sparse or economically unfeasible. Such integration is especially beneficial for civil engineering applications, such as foundation design, slope stability analysis, and groundwater resource assessment, where comprehensive knowledge of subsurface conditions is crucial. In summary, the integration of ERT with conventional geotechnical methods like the SPT provides a robust framework for subsurface characterization. While ERT alone cannot replace direct sampling techniques, it significantly enhances the spatial resolution of subsurface models and helps bridge the gaps between boreholes, leading to more informed decision-making in geotechnical and engineering applications. The successful correlation of ERT resistivity values with SPT N-values demonstrates the practical utility of hybrid approaches in subsurface investigations and reaffirms the value of multi-method strategies in modern geotechnical exploration.

Despite these encouraging results, several limitations should be acknowledged. The correlation model was developed using a limited number of boreholes, which may restrict the statistical robustness and spatial representativeness of the regression analysis. Furthermore, the established regression relationship is inherently site-specific, as resistivity–SPT correlations are strongly influenced by local lithology, groundwater conditions, and salinity levels; therefore, direct application to other geological settings should be undertaken with caution and may require recalibration. Future research could expand the dataset through additional boreholes and survey lines, apply three-dimensional ERT surveys to improve spatial resolution, and explore advanced analytical approaches such as machine-learning algorithms to develop more generalized predictive models. Overall, the integration of ERT with SPT provides a robust framework for subsurface characterization, reinforcing the value of multi-method strategies in modern geotechnical investigation while highlighting opportunities for methodological refinement and broader applicability.

Acknowledgement

The authors would like to thank the Universiti Tun Hussein Onn and Universiti Malaysia Pahang Al-sultan Abdullah for laboratory facilities, Southern Stars Solutions Pte. Ltd. for the technical assistance as well as additional financial support under UTHM Internal Research grants Q342.

Conflict of Interest

Authors declare that there is no conflict of interests regarding the publication of the paper.

Author Contribution

*The authors confirm contribution to the paper as follows: **study conception and design**: Z. M. Nizam, A. T. S. Azhar; **data collection**: Z. M. N. Hidayat, J. Amir; **analysis and interpretation of results**: Z. M. N. Hidayat, M. Aziman, I. M. Fakhrurrazi; **draft manuscript preparation**: Z. M. Nizam, H. Obiya, A. T. S. Azhar, Z. M. N. Hidayat. All authors reviewed the results and approved the final version of the manuscript.*

References

[1] Hossain, S., Kibria, G. & Khan, S. (2018). Site investigation using resistivity imaging. CRC Press. https://doi.org/10.1201/9781351047609

[2] Gonçalves, J. T. D., Botelho, M. A. B., Machado, S. L., & Netto, L. G. (2021) Correlation between field electrical resistivity and geotechnical SPT blow counts at tropical soils in Brazil, *Environmental Challenges*, *5*, 1-12. https://doi.org/10.1016/j.envc.2021.100220

[3] Yuxin, C., Arisa, K., Shinya, I. (2025) Prediction of Bearing Layer Depth Using Machine Learning Algorithms and Evaluation of Their Performance, *Machine Learning & Knowledge Extraction*, *7(3)*, 69. https://doi.org/10.3390/make7030069

[4] Hidayat, Z. M. N., Aziman, M., Azhar, A. T. S., Zainizan, S. (2019) Assessment of ground subsidence potential at problematic culvert on expressway: Case study using Electrical Resistivity Tomography (ERT) and Ground Penetrating Radar (GPR), *Journal of Applied Geoscience and Built Environment*, *1(1)*, 1-4.

[5] Dimech, A., Cheng, L., Chouteau, M., Chambers, J., Uhlemann, S., Wilkinson, P., Meldrum, P., Mary, B., Fabien-Oullet, G., Isabelle, A. (2022) A Review on Applications of Time-Lapse Electrical Resistivity Tomography Over the Last 30 Years: Perspectives for Mining Waste Monitoring, *Surveys in Geophysics*, *43*, 1699-1759. https://doi.org/10.1007/s10712-022-09731-2

[6] Kaitian, L., Jianbo, Y., Fan, L., Yongpeng, Y., Yulin, L., Lin, Z., Peng, W., Zhenyu, L., Yancheng, Y., Jianweng, W. (2024) Non-invasive geophysical methods for monitoring the shallow aquifer based on time-lapse electrical resistivity tomography, magnetic resonance sounding, and spontaneous potential methods, *Scientific Reports*, *14*, 7320, 1-12. https://doi.org/10.1038/s41598-024-58062-2

[7] M. S. I. Zaini, M. F. Ishak, M. F. Zolkepli, M. S. Wahap, J. I. Jaafar Sidek, A. Mohd Yasin, M. N. Zolkepli, M. H. Mohmad Sidik, K. Z. Mohd Arof, Z. Abu Talib (2020) Granite exploration by using Electrical Resistivity Imaging (ERI): A case study in Johor, *International Journal of Integrated Engineering*, *12(8)*, 328-347. https://doi.org/10.30880/ijie.2020.12.08.032

[8] Syazwan, A. S., Azhar, S. A. T., Mohammad, I. S. A., Hidayat, Z. M. N., Nordiana, M. M. (2021) Groundwater pathway mapping using Electrical Resistivity Tomography (ERT) method, *Journal of Sustainable Underground Exploration*, *1(1)*, 32-37, https://doi.org/10.30880/jsue.2021.01.01.005

[9] Chibuze, G. C., Joshua, U. N., Adegoke, I. A. (2024) Comprehensive review of groundwater assessment techniques: Enhancing subsurface understanding through integrated methods, *Pakistan Journal of Geology*, *8(1)*, 57-66. https://doi.org/10.26480/pjg.01.2024.57.66

[10] Qiang, G., Yanjun, S., Muhammad, H., Weijun, J., Peng, Y. (2018) Evaluation of a Weathered Rock Aquifer Using ERT Method in South Guangdong, China, Water, *10(3)*, 293, 1-22. https://doi.org/10.3390/w10030293

[11] Jiaqi, W., Fuchu, D., Zhiquan, H., Lingchao, M. (2023) Application of the electrical resistivity tomography in groundwater detection on loess plateau, *Scientific Reports*, *13*, 4821, 1-14. https://doi.org/10.1038/s41598-023-31952-7

[12] Miaojun, S., Qianlong, Z., Honglei, S., Zhenqi, W. (2023) Experimental Study on Axial Stress and Hammer Impacting Energy of Offshore Standard Penetration Test, *Applied Sciences*, *13(17)*, 1-14. https://doi.org/10.3390/app13179487

[13] Zhdanov, M., Keller, G. (1994) The Geoelectrical methods in geophysical exploration, *International Journal of Rock Mechanics and Mining Sciences & Geomechanics Abstracts*, *31(4)*, 873. https://doi.org.10.1016/0148-9062(94)91092-8

[14] Zhou, B. (2018) Electrical Resistivity Tomography: A Subsurface-Imaging Technique, Applied Geophysics with Case Studies on Environmental, *Exploration and Engineering Geophysics*, 1-16. https://doi.org/10.5772/intechopen.81511

[15] Sang, M. G. P. P., Nita, A. (2024) Correlation of CPT, SPT, and ERT data for a better understanding of soils condition: A case study in SPG Merbau, South Sumatra, *IOP Conference Series Earth and Environmental Science*, 1-13. https://doi.org/10.1088/1755-1315/1416/1/012008

[16] Juliana, T. D. G., Marco, A. B. B., Sandro, L. M., Leonides, G. N., Peng, Y. (2021) Correlation between field electrical resistivity and geotechnical SPT blow counts at tropical soils in Brazil, *Environmental Challenges*, *5*, 1-12. https://doi.org/10.1016/j.envc.2021.100220

[17] Sudha, K., Israil, M., Mittal, S., Rai, J. (2009) Soil characterization using electrical resistivity tomography and geotechnical investigation, *Journal of Applied Geophysics*, *67(1)*, 74-79. https://doi.org/10.1016/j.jappgeo.2008.09.012

[18] Siddiqui, F.I., Osman, S.B.A.B.S. (2013) Simple and multiple regression models for relationship between electrical resistivity and various soil properties for soil characterization, *Environmental Earth Science*, *70*, 259-267. https://doi.org/10.1007/s12665-012-2122-0

[19] Zeinab, A., Samsudin, A. R., Yaacob, W. Z., Jasni, Y. (2012) Groundwater investigation using electrical resistivity imaging technique at Sg. Udang, Melaka, Malaysia, *Bulletin of the Geological Society of Malaysia*, *58*, 55-58.

[20] Schwartz, M. O., Rajah, S. S., Askury, A. K., Putthapiban, P., Djaswadi, S. (1995) The Southeast Asian Tin Belt, *Earth-Science Review*, *38*, 95-293.

[21] Lundström, K., Larsson, R., Dahlin, T. (2009) Soil characterization using electrical resistivity tomography and geotechnical investigation, *Landslides*, *6(1)*, 1-15. https://doi.org/10.1007/s10346-009-0144-9

[22] Groves, P., Cascante, G., Dundas, D., Chatterji, P.K. (2011) Use of geophysical methods for soil profile evaluation, *Canadian Geotechnical Journal*, *48(9)*, 1364-1377. https://doi.org/10.1139/t11-044

[23] Ward, S.H. (1990) *Resistivity and Induced Polarization Methods*, Geotechnical and Environmental Geophysics: Volume I, Review and Tutorial. https://doi.org/10.1190/1.9781560802785.ch6

[24] Martorana, R., Fiandaca, G., Casas Ponsati, A., Cosentino, P.L. (2009) Comparative tests on different multi-electrode arrays using models in near-surface geophysics, *Journal of Geophysics and Engineering, 6(1)*,1-20. https://doi.org/10.1088/1742-2132/6/1/001

[25] Sufiyanussuari, S. A., Ahmad Tajudin, S. A., Azmi, M. I. S., Zahari, M. N. H., & Mohd Muztaza, N. (2021) Groundwater Pathway Mapping Using Electrical Resistivity Tomography (ERT) Method, *Journal of Sustainable Underground Exploration*, *1(1)*, 32-37. https://doi.org/10.30880/jsue.2021.01.01.005

[26] Z. M. Nizam, A. T. S. Azhar, M. Aziman, Z. M. N. Hidayat, J. A. Aziz, N. M. N. Amri (2024) Assessing the Impact of Lithological and Geological Features on Electrical Resistivity Tomography (ERT) at Kelantan River Basin, Malaysia, *International Journal of Integrated Engineering*, *16(4)*, 113-123. https://doi.org/10.30880/ijie.2024.16.04.014

[27] Melvern, G. K. H., Aziman, M., Khaidir, M. A. T., Faizal, P., Firdaus, M. M. D., Niza, S. M, Z. M. Nizam, Azhar, A. T. S., Badee, A. (2026) Apparent Electrical Resistivity Value and Borehole Data Correlation, *Journal of Advanced Research in Applied Sciences and Engineering Technology*, *56(2)*, 197-205. https://doi.org/10.37934/araset.56.2.197205

[28] Keller, G. V. & Frischknecht, F. C. (1966) *Induction and galvanic resistivity studies on the Athabasca Glacier, Alberta, Canada*. Geology of the Arctic. https://doi.org/10.3138/9781487584962-007

[29] Netto, L. G., Filho, W. M., Moreira, C. A., Donato, F. T., Helene, L. P. I. (2021) Delineation of necroleachate pathways using electrical resistivity tomography (ERT): Case study on a cemetery in Brazil, *Environmental Challenges*, *5*, 1-12. https://doi.org/10.1016/j.envc.2021.100344

[30] Devi, A., Israil, M., Anbalagan, R., Gupta, P.K. (2017) Subsurface soil characterization using geoelectrical and geotechnical investigation at bridge site in Uttarakhand Himalayan region, *Journal of Applied Geophysics*, *144*, 78-85. https://doi.org/10.1016/j.jappgeo.2017.07.005